ISSN 1062-8738, Bulletin of the Russian Academy of Sciences. Physics, 2013, Vol. 77, No. 11, pp. 1386–1390. © Allerton Press, Inc., 2013.
Original Russian Text © O.A. Kogtenkova, P. Zieba, T. Czeppe, L. Lityn'ska-Dobrzynska, B.B. Straumal, A.N. Nekrasov, 2013, published in Izvestiya Rossiiskoi Akademii Nauk. Seriya Fizicheskaya, 2013, Vol. 77, No. 11, pp. 1681–1686.

Wetting of Grain Boundaries by the Second Solid Phase in Al-Based Alloys

O. A. Kogtenkova[a], P. Zieba[b], T. Czeppe[b], L. Lityn'ska-Dobrzynska[b], B. B. Straumal[a], and A. N. Nekrasov[c]

[a] *Institute of Solid-State Physics, Russian Academy of Sciences, Chernogolovka, Moscow oblast, 142432 Russia*
[b] *Institute of Metallurgy and Materials Science, Polish Academy of Sciences, Cracow, 30-059 Poland*
[c] *Institute of Experimental Mineralogy, Russian Academy of Sciences, Chernogolovka, Moscow oblast, 142432 Russia*
e-mail: koololga@issp.ac.ru

Abstract—This work presents data on changes in the structure and properties of aluminum-based alloys subjected to severe plastic deformation by high-pressure torsion. Microstructure and the composition and change in temperature for phases are studied for double (Al–Zn, Al –Mg) and ternary (Al–Mg–Zn) alloys. Tie-lines of the liquid phase wetting of grain boundaries and grain boundary solvus lines are constructed on phase diagrams of our Al–Zn and Al–Mg systems. The shifting of the phase composition in the bulk of aluminum grains from the Al + τ region to the Al + η region of the Al–Mg–Zn phase diagram with an increase in the specific area of grain boundaries is described.

DOI: 10.3103/S1062873813110166

INTRODUCTION

Al–Zn, Al–Mg, and Al–Mg–Zn systems are basic to the production of materials that are widely used in a variety of technical fields. Investigations of the grain boundary (GB) phase transitions in these systems enable us not only to contribute to our understanding of the physical foundations of such processes, but help in the development of new materials to meet the needs of modern industry as well.

Cahn was the first to predict the existence of a phase transition upon the wetting of interfaces [1]; i.e., the grain boundary can contain thin stable layers of the second phase that are unstable in the bulk. Such thin layers are often referred to as grain boundary phases. They are observed in multicomponent oxides [2], silicon nitride [3]; and Nd–Fe–B, Fe–Cu–Nb–Si–B, and Fe–Zr–Cu–B nanocrystalline materials with magnetic properties [4–6]. Nevertheless, the true nature of GB layers and the thermodynamic conditions for their formation in many cases remain unknown. GB phase transitions are therefore of ever-growing interest, especially now that nanocrystalline materials have became one of the most promising trends in the development of material science. Because these materials have small grain sizes and a considerable fraction of the atoms in them are found on GBs, their properties can change radically as a result of GB phases.

Conditions for the equilibrium GB phase in the single-phase region of the bulk phase diagram depend substantially on the conditions for GB transitions in the two-phase region (Fig. 1). Let us analyze the GB phase transition of wetting by the liquid phase. The wetting depends on GB energy σ_{GB}. We consider contact angle θ between the material with the GB and the liquid phase. When σ_{GB} is lower than $2\sigma_{SL}$, where σ_{SL} is the energy of the interface between the liquid and

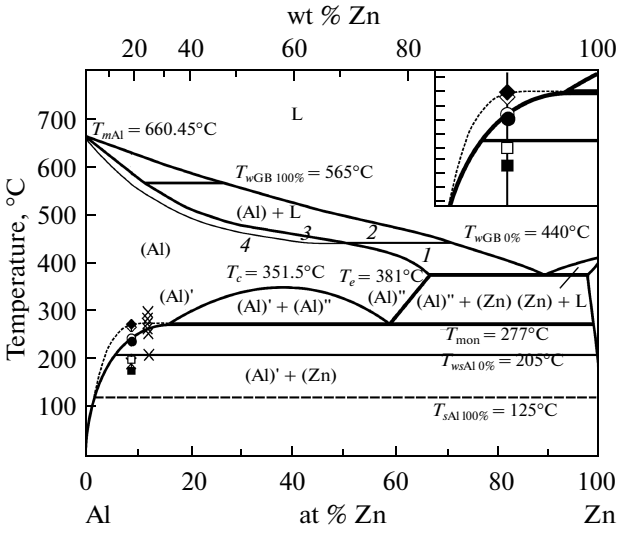

Fig. 1. Al–Zn phase diagram with tie-lines of phase wetting transition. Solid lines show the phase transitions in the volume. The fine and dotted lines indicate grain boundary phase transitions. The vertical fine line at 20 wt % Zn identifies the studied composition. The insert with the enlarged scale shows the investigated range of temperatures and concentrations upon HPT for samples heated in the DSC. The white symbols correspond to a DSC rate of 10 K min^{-1}; the black ones, to a rate of 20 K min^{-1}. Crosses denote the experimental points for cast alloys [16].

solid phases, the GB is wetted incompletely, and $\theta > 0°$ (point *1* on the Al–Zn phase diagram in Fig. 1). However, when $\sigma_{GB} \geq 2\sigma_{SL}$, the GB is wetted completely, and contact angle $\theta = 0°$ (point *2*). Since the curves describing temperature dependences $2\sigma_{SL}$ and σ_{SL} intersect, the GB wetting phase transition occurs at some temperature T_W. Contact angle $\theta = 0°$ lies at $T \geq T_W$. The tie-line of the GB wetting phase transition appears at T_W in the S + L region of the bulk phase diagram. The liquid phase becomes metastable at the intersection with the bulk solidus between points *2* and *3*. Its occurrence at the grain boundary causes energy loss Δg. The energy gain $(\sigma_{GB} - \sigma_{SL})$ of T_W can stabilize the liquid-like GB layer with thickness *l*. Moving from two-phase region S + L into single-phase region S of the bulk phase diagram (from point *2* to point *3*), energy loss Δg caused by the formation of a metastable quasi-liquid layer increases. Liquid-like GB layers disappear near the GB solidus, where Δg is equal to $\sigma_{GB} - \sigma_{SL}$. A stable liquid-like phase layer (unstable in the bulk) can therefore exist at the GB between the lines of the bulk and GB solidus (point *3*). The GB at point *4* is clear and contains only the usual adsorption layer of the second component. Temperature T_W depends on GB energy σ_{GB}. GBs with high σ_{GB} values have low T_W. In the S + L region above the minimum T_W lies the family of tie-lines of GB wetting for the maximum σ_{GB}. These tie-lines of the phase wetting transition spread, as does the family of GB solidus lines in the single-phase region S.

The transition from incomplete to complete wetting of the GB by the liquid phase always proceeds with an increase in temperature [7–9], since the specific excess free energy σ_{SL} of the solid and liquid phase boundary always falls with the temperature more quickly than σ_{GB} at the interface of two solid phases. When the wetting phase is solid, the transition from incomplete wetting of the GB to complete wetting can occur with a rise [9] and a drop in temperature [10]. The aim of this work was to investigate the transition of phase wetting by the second solid phase in aluminum-based alloys cast and deformed by high-pressure torsion (HPT).

EXPERIMENTAL

Alloys based on aluminum Al–(19, 20, 30 wt %) Zn, Al–(5, 10, 15, 18, 25 wt %) Mg, and Al–(2, 4 wt %) Mg–(5, 10 wt %) Zn were smelted from high-purity components (5*N*5 Al, 5*N* Zn, and 4*N*5 Mg) in a vacuum induction furnace. Our experiments were performed with disks 2 mm in diameter, cut from a cylindrical ingot of aluminum alloy with a diameter of 10 mm. The cast disks of this alloy, refined by chemical etching, were subjected to high-pressure torsion deformation at room temperature under a pressure of 5 GPa in Bridgman anvils (five revolutions with a speed of 1 rpm). Samples 3 mm in diameter were cut from the middle of the radii of HPT-deformed disks for structural studies and calorimetric measurements. Investigations were conducted in two steps. At the first step, the cast alloys were annealed in a Snol 6.7/1300 electric furnace at temperatures of 100 to 300°C with intervals of 50°C for 4000 h. At the second step, the cast and deformed samples were heated in a differential scanning calorimeter (DSC) from room temperature up to 350°C with rates of 10 and 20 K min^{-1}.

The alloy samples before and after deformation were investigated by differential scanning calorimetry on TA Instruments 910 and 1600 calorimeters, transmission electron microscopy (TEM) on a Philips CM 20 microscope under an accelerating voltage of 200 kV, and scanning electron microscopy (SEM) on a Philips XL30 scanning microscope equipped with a LINK ISIS Oxford Instrument energy dispersive spectrometer.

RESULTS AND DISCUSSION

Based on data of X-ray structural analysis and electron microscopy investigations, it was shown that the structure of all the studied Al–Zn, Al–Mg, and Al–Mg–Zn alloys contained the aluminum-based solid solution [11]. The Al–Zn alloys before and after deformation are two-phases; (Al) and (Zn) solid solutions are present within them. The structure of Al–Mg alloys both in the as-cast and in deformed state contains the β (Al_3Mg_2) intermetallide phase [12]. The cast undeformed Al–Zn–Mg alloys contain the fine particles of $Mg_{32}(Al,Zn)_{49}$ (τ-phase), $MgZn_2$ (η phase), $AlMg_4Zn_{11}$ (η' phase), and Mg_7Zn_3 phases embedded in the matrix of (Al) aluminum-based solid solution. Particles of (τ, η phase), (η' phase), and Mg_7Zn_3 phases fully dissolved as a result of the severe plastic deformation (SPD).

The severe plastic deformation results in a strong increase in the grain size and the dissociation of oversaturated solid solution in alloys studied. The grain size becomes less by two–three orders than in cast alloys. Particles of intermetallides and Zn, whose size is around 10 nm, are uniformly distributed over the material bulk. The probable mechanism of the dissociation of oversaturated solid solution is GB diffusion accelerated by the flow of nonequilibrium vacancies.

At the first step, we investigated cast alloys with a grain size around 500 μm. The aim of this investigation was the determination of the phase transition temperature for wetting by the second solid phase in the low-temperature region on bulk phase diagrams of Al–Zn and Al–Mg alloys.

Let us consider in more detail each of these systems.

Al–Mg Alloys

Experiments were performed with Al–Mg polycrystals with a second component percentage of 10, 15, 18, and 25 wt % Mg, which were annealed for 4000 h in the two-phase region of the phase diagram.

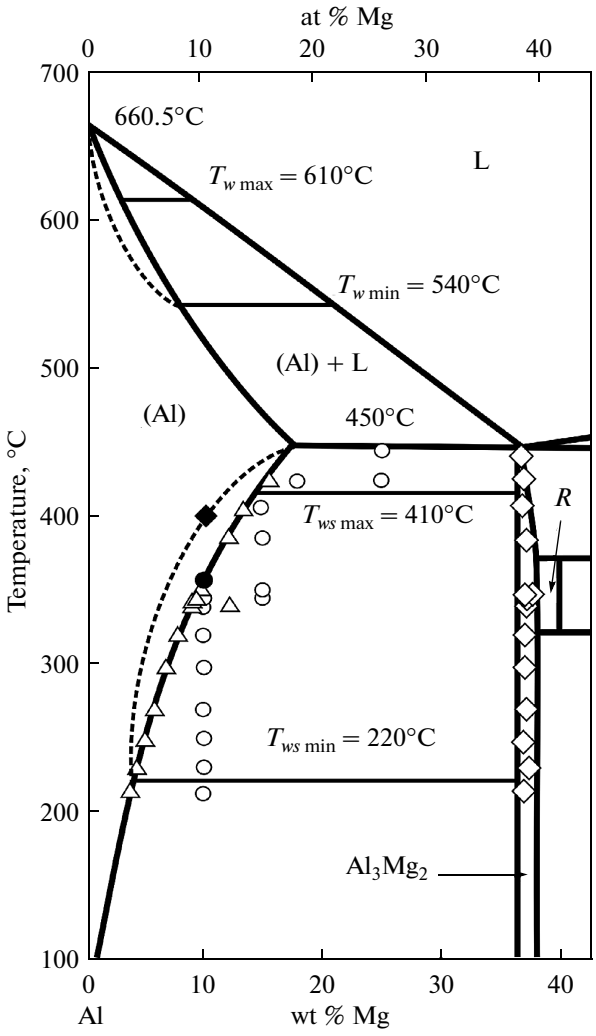

Fig. 2. Al–Mg phase diagram with the tie-lines of phase wetting transitions. Solid lines show the phase transitions in the volume. The thin and dotted lines denote grain boundary phase transitions. The white symbols correspond to experimental points for cast alloys; the black ones, the points for deformed alloys heated in DSC [13].

The temperature of the beginning of the GB phase transition corresponds to $T_{ws\,min} = 220 \pm 5$°C (Fig. 2). Particles of the Al_3Mg_2 phase form chains along Al/Al grain boundaries above this temperature; however, not all the Al/Al grain boundaries are completely wetted by the layer of the Al_3Mg_2 phase. The contact angle between Al_3Mg_2 particles and Al/Al grain boundaries is small, but no zero. The GBs wetted by the second phase are not observed below $T_{ws\,min}$. As the temperature rises, the amount of Al/Al boundaries wetted completely by the Al_3Mg_2 phase increases. All the Al/Al boundaries are completely wetted by the Al_3Mg_2 phase above the maximum temperature for the GB phase wetting transition, $T_{ws\,max} = 410 \pm 5$°C, and are divided each other by the continuous Al_3Mg_2 layer. The thickness of the wetting Al_3Mg_2 layer depends on the amount of the phase and rises with increasing the magnesium content in the alloy. Thus, the fraction of wetted grain boundaries between $T_{ws\,min}$ and $T_{ws\,max}$ increases as the temperature rises from 0 up to 100%.

Al–Zn Alloys

The wetting of grain boundaries by the solid phase was observed in the Al–Zn system as well as in the Al–Mg system. However, if the transition from the incomplete wetting of grain boundaries to complete that occurs in the Al–Mg system with an increase in temperature as at the liquid-phase wetting, so this transition in the Al–Zn system occurs with a reduction in temperature.

Experiments were performed using Al–Zn polycrystals with a second component percentage of 10, 20, and 30 wt % Zn, annealed for 1000–4000 h below the monotectoidal temperature $T_{mon} = 277$°C.

In our investigations, we measured average contact angle θ between the (Al)/(Al) grain boundaries and the grain-boundary particles of the (Zn) phase in polycrystals. As the temperature fell, so did θ. It was thus determined that the temperature for the complete wetting of grain boundaries by the second solid phase (where Al/Al GBs are completely covered by solid layers of zinc) in Al–Zn alloys was $T_{wsAl\,100\%} = 125 \pm 5$°C (Fig. 1). No GBs wetted by the second phase were observed at temperatures above $T_{wsAl\,0\%} = 205 \pm 5$°C. As a result, new tie-lines of the GB phase transformations were constructed on our Al–Zn and Al–Mg bulk phase diagrams (Fig. 1, 2).

At the second step of our investigations, we studied cast (grain size of 500 μm) and deformed (grain size of 100–200 nm) Al–Zn, Al –Mg, and Al–Mg–Zn alloys by means of differential scanning calorimetry.

Let us consider in detail each of these systems.

Al–Zn Alloys

We investigated the Al–20 wt % Zn alloy before and after HPT at heating rates of 10 and 20 K min^{-1} in a differential scanning calorimeter. The redistribution of zinc localized after HPT in the triple junctions of (Al) grains in layers along (Al)/(Al) grain boundaries is due to the tendency of these boundaries to be completely wetted by zinc layers. The grains were coarse (up to 0.5 mm) in experiments of the first step, and the boundaries during annealing were immovable. The redistribution of zinc over the aluminum grain boundaries consequently required diffusion over large distances and the longest times for annealing. At any given step with submicron grain size, they continued to grow during annealing. Shorter diffusion paths and boundary migration during grain growth simplified the formation of equilibrium wetting layers of zinc at the grain boundaries within aluminum (as the moderate migration of grain boundaries facilitated the formation of their equilibrium faceting [3, 4]).

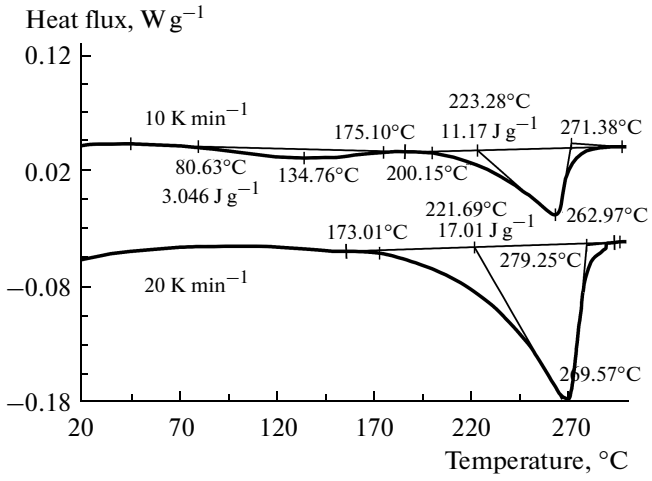

Fig. 3. DSC curves for Al–20 wt % Zn alloy after HPT at 10 and 20 K min^{-1}.

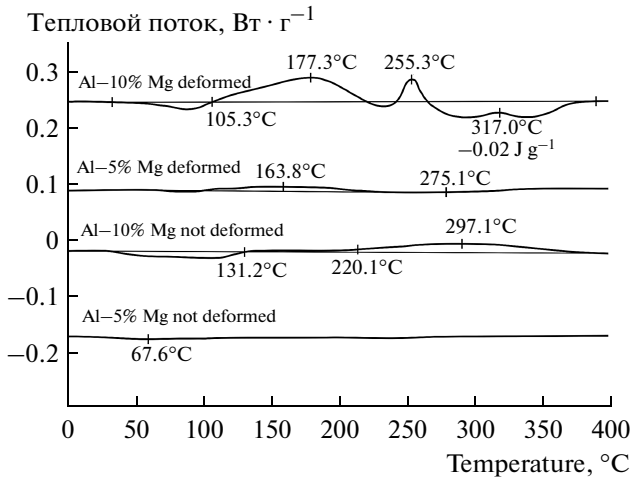

Fig. 4. DSC curves for Al–5 wt % Mg and Al–10 wt % Mg alloys before and after deformation.

Using the standard methods for interpreting DSC curves [14], three points can be noted on the curves in Fig. 3. The minimum at 263.0°C (10 K min^{-1}) and 269.6°C (20 K min^{-1}) corresponds to the termination of the exothermic reaction (the diamonds in Fig. 3). The temperature of the onset of the exothermic reaction can be obtained if we draw a tangent to the DSC curve from the minimum point in the direction of low temperatures up to its intersection with the base lines [14]. This intersection lies at 223.3°C (10 K min^{-1}) or 221.7°C (20 K min^{-1}). These values are not only close to one another, but also coincide with the point at the line of the solubility limit (solvus) for the investigated Al–20 wt % Zn alloy (marked with circles on the phase diagram in Fig. 3). The point of the tangent's intersection with the base line for our single-step exothermic reaction virtually coincides with the temperature where the DSC curve begins to turn down from the base line [14]. In our case, this process began much earlier at 202.2°C (10 K min^{-1}) and 173.0°C (20 K min^{-1}), respectively (the squares in Fig. 3). This means that the observed exothermic reaction consisted of at least two steps. Moreover, during heating at a rate of 10 K min^{-1}, one more low and wide minimum is observed on the DSC curve between 80.6 and 175.1°C. It is invisible on the curve recorded at a rate of 20 K min^{-1}, where it probably merged with the principal minimum that occured here much earlier (at 173.0°C) than upon heating at a rate of 10 K min^{-1} (202.2°C).

The processes observed on DSC curves below 200°C were associated with the redistribution of zinc particles into wetting layers over grain boundaries, and with the partial dissolution of zinc in the aluminum grain bulk. With further heating above 200°C, the exothermic reaction of the complete dissolution of zinc in aluminum (Zn + Al → (Al)), continued. It should have been complete at a solvus temperature of ~223°C (the circles in Fig. 1), but this did not happen; the reaction continued and finished only at 263–270°C (the diamonds in Fig. 1). The position for the line of the grain boundary solvus for Al–20 wt % Zn was thus determined successfully for the first time (Fig. 1). Samples not deformed behaved like deformed ones at 10 K min^{-1}.

Al–Mg Alloys

Al–Mg alloys with second components of 5 and 10 wt % were investigated by differential scanning calorimetry before and after HPT. The minimum at 275.1°C on the DSC curves (Fig. 4) was observed for samples of Al–5 wt % Mg alloy after deformation. The temperature of 275.1°C lay 25°C above that of the bulk solvus line on the phase diagram (Fig. 1). This could indicate that the dissolution of particles of the Al_3Mg_2 second phase on the grain boundaries occurred above the bulk solvus line (the process was already complete at 241.2°C). No second phase layers were observed at 400°C. According to the data from transmission electron microscopy, our Al–10 wt % Mg alloys (both deformed and not deformed) heated in the DSC from 20 to 400°C also showed layers of the Al_3Mg_2 second phase on GBs above the bulk solvus at 400°C.

The position of the line of the grain boundary solvus for Al–Mg was thus successfully determined for the first time.

Al–Mg–Zn Alloys

Ternary Al– 4 wt % Mg–10 wt % Zn and Al– 2 wt % Mg–5 wt % Zn were investigated before and after deformation [15]. The undeformed cast alloys contained fine particles of $Mg_{32}(Al,Zn)_{49}$ (τ phase), $MgZn_2$ (η phase), $AlMg_4Zn_{11}$ (η' phase), and Mg_7Zn_3 phases embedded in a matrix of aluminum-based solid solu-

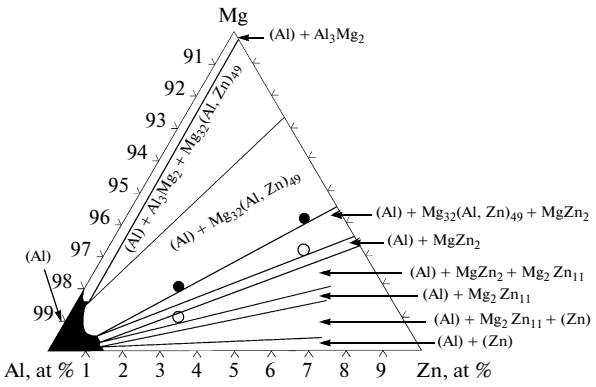

Fig. 5. Ternary Al–Mg–Zn phase diagram at 25°C [17]. Black dots correspond to the composition of the investigated alloys; white dots, to the calculated composition for internal grains with GB adsorption in a Mg monolayer and GB adsorption without Zn for grains 150 nm in size.

tion. All of the phases dissolved around 148°C during heating in the DSC, and τ nanoparticles coherent with the (Al) matrix formed at a temperature of ~222°C. The HPT of cast alloys strongly changes the grains of (Al) solid solution from 500 μm to 120–150 nm. Particles of the τ, η, η', and Mg_7Zn_3 phases embedded in the matrix of an Al-based solid solution completely dissolve upon severe plastic deformation. As a result of heating a nanograin solid solution, an Al-based η phase forms, and its bulk fraction grows as the temperature rises. Since magnesium is adsorbed at grain boundaries more than zinc, the phase composition in the (Al) grain bulk of nanograin samples shifts the ternary Al–Mg–Zn phase diagram from the (Al) + τ region into the (Al) + η region (Fig. 5).

CONCLUSIONS

(1) Tie-lines for the phase wetting transition in Al–Zn and Al–Mg systems have been constructed.

(2) Grain boundary solvus lines in the (Al) single-phase region on Al–Zn and Al–Mg phase diagrams have been constructed.

(3) Precipitates of the second phase were observed on grain boundaries above the bulk solvus lines in our Al–Zn and Al–Mg systems.

(4) The HPT of Al–Mg–Zn alloy completely dissolves fine particles of the τ, η, η', and Mg_7Zn_3 phases embedded in the matrix of an Al-based solid solution.

(5) In heating cast samples of Al–Mg–Zn alloy, the nonequilibrium τ, η, η', and Mg_7Zn_3 phases dissolved while particles of the equilibrium τ phase grew. In contrast, an Al-based η phase formed as a result of heating the nanograin solid solution and grew as the temperature rose.

(6) The phase composition in the (Al) grain bulk shifted on the ternary Al–Mg–Zn phase diagram from the (Al) + τ region into the (Al) + η region.

REFERENCES

1. Cahn, J.W., *J. Chem. Phys.*, 1977, vol. 66, p. 3667.
2. Onreabroy, W., Sirikulrat, N., Brown, A.P., et al., *Solid State Ionics,* 2006, vol. 177, p. 411.
3. French, R.H., Mullejans, H., Jones, D.J., et al., *Acta. Mater.*, 1998, vol. 46, p. 2271.
4. Hosseini, H.R.M. and Kianvash, A., *J. Magn. Magn. Mater.*, 2004, vol. 281, p. 92.
5. Yue, M., Zhang, J.X., and Liu, W.Q., *J. Magn. Magn. Mater.*, 2004, vol. 271, p. 364.
6. Betancourt, I. and Davies, H.A., *J. Magn. Magn. Mater.*, 2003, vol. 261, p. 328.
7. Eustathopoulos, N., *Int. Met. Rev.,* 1983, vol. 28, p. 189.
8. Straumal, B., Muschik, T., Gust, W., et al., *Acta. Metal. Mater.*, 1992, vol. 40, p. 939.
9. Straumal, B., Molodov, D., and Gust, W., *Interface Sci.*, 1995, vol. 3, p. 127.
10. Protasova, S.G., Kogtenkova, O.A., Straumal, B.B., et al., *J. Mater. Sci.,* 2011, vol. 46, p. 4349.
11. Mazilkin, A.A., Kogtenkova, O.A., Straumal, B.B., et al., *Def. Diff. Forum*, 2005, vols. 237–240, p. 739.
12. Mazilkin, A.A., Straumal, B.B., Protasova, S.G., et al., *Fiz. Tverd. Tela*, 2007, vol. 49, no. 5, p. 826.
13. Straumal, B.B., Baretzky, B., Kogtenkova, O.A., et al., *J. Mater. Sci.,* 2010, vol. 45, p. 2057.
14. Dean, J.A., *The Analytical Chemistry Handbook*, New York: McGraw-Hill, 1995.
15. Kogtenkova, O.A., Mazilkin, A.A., Straumal, B.B., et al., *J. Mater. Sci.,* 2013, vol. 48. issue 13, pp. 4758–4765. DOI: 10.1007/s10853-013-7266-0.
16. Protasova, S.G., Kogtenkova, O.A., Straumal, B.B., et al., *J. Mater. Sci.*, 2011, vol. 46, p. 4349.
17. *Handbook of Ternary Alloy Phase Diagrams*, Villars, P., Prince, A., and Okamoto, H., Eds., Metals Park, OH: ASM Int., 1995.

Translated by S. Ordzhonikidze

SPELL: 1. faceting, 2. occured